J. Anat. (1999) **194**, pp. 51–60 with 8 figures Printed in the United Kingdom

Morphometric studies of secretory granule formation in mouse pancreatic acinar cells. Dissecting the early structural changes following pilocarpine injection

ILAN HAMMEL[1], OSNAT SHOR-HAZAN[1], TORA ELDAR[1], DINA AMIHAI[1] AND SYLVIA LEW[1,2]

[1] *Department of Pathology Sackler Faculty of Medicine, Tel-Aviv University, Ramat-Aviv, Tel-Aviv, Israel and*
[2] *Institute of Pathology, Meir Hospital, Kfar-Sava, Israel*

(*Accepted 15 September 1998*)

ABSTRACT

Secretory granule formation in pancreatic acinar cells is known to involve massive membrane flow. In previous studies we have undertaken morphometry of the regranulation mechanism in these cells and in mast cells as a model for cellular membrane movement. In our current work, electron micrographs of pancreatic acinar cells from ICR mice were taken at several time points after extensive degranulation induced by pilocarpine injection in order to investigate the volume changes of rough endoplasmic reticulum (RER), nucleus, mitochondria and autophagosomes. At 2–4 h after stimulation, when the pancreatic cells demonstrated a complete loss of granules, this was accompanied by an increased proportion of autophagosomal activity. This change primarily reflected a greatly increased proportion of profiles retaining autophagic vacuoles containing recognisable cytoplasmic structures such as mitochondria, granule profiles and fragments of RER. The mitochondrial structures reached a significant maximal size 4 h following injection (before degranulation 0.178 ± 0.028 μm^3; at 4 h peak value, 0.535 ± 0.109 μm^3). Nucleus size showed an early volume increase approaching a maximum value 2 h following degranulation. The regranulation span was thus divided into 3 stages. The first was the membrane remodelling stage (0–2 h). During this period the volume of the RER and secretory granules was greatly decreased. At the intermediate stage (2–4 h) a significant increase of the synthesis zone was observed within the nucleus. The volume of the mitochondria was increasing. At the last step, the major finding was a significant granule accumulation in parallel with an active Golgi zone.

Key words: Mitochondria; endoplasmic reticulum; autophagosomes; zymogen granule synthesis.

INTRODUCTION

The sequence of the cellular events leading to the formation of pancreatic acinar granules has been extensivey studied (Farquhar & Palade, 1981; Castle et al. 1987; Pfeffer & Rothman, 1987). Secretory components are packed in the Golgi complex (GC), the progranules bud-off the transcisternae and then fuse to form an immature granule, i.e. the condensing vacuole. The latter changes its morphology and transforms into a mature electron-dense granule. The steps in granule formation involve massive membrane shuttling, a process which may be expressed in changes in the structure of internal organelles. The model of immature granule formation via progranule fusion, although generally accepted, is based primarily on qualitative analysis of electron micrographs demonstrating apparent fusion of progranules, and on pulse-label autoradiographic studies showing the appearance of label, first in progranules, then in condensing vacuoles and finally in mature granules (Farquhar & Palade, 1981; Darnell et al. 1990; Hammel et al. 1998).

One of the earliest steps in secretory granule formation is thought to consist of the synthesis of secretory proteins inside the rough endoplasmic reticulum (RER). Those newly formed proteins are usually in the preprotein form. While moving to the exit side a peptide is dissected to form a proprotein. Other chemical modifications may occur in RER such

Correspondence to Dr Ilan Hammel, Department of Pathology, Sackler Faculty of Medicine, Tel Aviv University, Ramat-Aviv, Tel-Aviv 69978, Israel. e-mail: ilanh@patholog.tau.ac.il

as glycosylation to form a glycoprotein. Only the proprotein enters the GC (Farquhar & Palade, 1981; Darnell et al. 1990). Little is known about the structural changes in RER during secretory protein synthesis. One possible approach to gaining more knowledge in this area is to examine the changes in morphology of the RER system using quantitative microscopy techniques. Following pilocarpine injection, Okano & Nakamura (1965) noted a vesicular transformation of the RER within 15 min of injection. Watari & Baba (1968) found degenerating mitochondria and formation of autophagic vacuoles in dog pancreas 1–3 h after pilocarpine administration, while Nevalainen (1970) found no significant changes in the size and content of mitochondria in rat pancreatic acinar cells following pilocarpine injection. Both groups noted that the autophagic vacuoles contained recognisable cytoplasmic structures such as mitochondria and fragments of RER.

In the present study we have used a morphometric approach to analyse changes in the lumen size within the RER in pancreatic acinar cells after pilocarpine-stimulated secretion. We found that 4 h following complete cell degranulation a significant decrease in the internal volume of the RER is seen. At that time point there is an increase in mitochondrial volume as well as the accumulation of a significant number of autophagosomes. Taken together, these findings support the hypothesis that pancreatic acinar cell regranulation is a result of a significant membrane turnover (Darnell et al. 1990).

MATERIALS AND METHODS

Treatment of mice. Adult female ICR mice (aged 9–10 wk, body weight 20–25 g.) were maintained on a diet of standard rodent chow (Mabaroth, Israel) and tap water ad libitum. For these experiments, food was withheld overnight, and then some of the mice were injected i.p. with pilocarpine (2.0 mg/mouse in 0.2 ml 0.9% NaCl; Sigma, St Louis, Missouri) to induce pancreatic acinar cell degranulation (Covell, 1928). Groups of 5 animals were killed before or at 1, 2, 4, 8, 17 or 27 h after injection with pilocarpine. The dose of pilocarpine and the intervals of sampling were selected based on preliminary studies in which the extent of pancreatic acinar cell degranulation was assessed in light microscopic sections and resulted in more than 95% degranulation (Weintraub et al. 1992; Lew et al. 1994). Besides inducing exocytosis in the pancreas it is known to cause lacrimation and fluid and electrolyte loss. The animal experiments were conducted in accordance with the Tel Aviv University Institutional Animal Care and Use Committee and with guidelines prepared by the Committee on the Care and Use of Laboratory Animals of the Institute of Laboratory Animal Resources, National Research Council (DHH Publication No. 86–23, revised 1985).

Tissue preparation. Mice were killed by cervical dislocation. The pancreas was removed immediately and diced into small pieces ($< 1\ mm^3$) which were fixed for 2 h at room temperature in 2.5% glutaraldehyde, 0.8% paraformaldehyde, and 0.025% $CaCl_2$ in 0.1 M sodium cacodylate buffer (pH 7.4). After fixation, the tissue was postfixed in 1% osmium tetroxide (in 0.1 M sodium cacodylate buffer), dehydrated in a graded series of alcohols and embedded in Poly-Bed 812 resin kit (Polyscience, Warrington, USA). Several blocks (at least 5) were prepared from each pancreas and for each mouse the first 2 blocks in the storage box were chosen for electron microscopy. The ultrathin sections ($0.075 \pm 0.015\ \mu m$), contrasted with uranyl acetate and lead citrate, were observed using a JEOL 100B transmission electron microscope.

Quantitative microscopy. Morphometry was performed on randomly obtained electron micrographs (X12,000) of pancreatic cells as previously described in detail (Hammel et al. 1987, 1989; Weintraub et al. 1992; Lew et al. 1994). In short, systematic sampling of the sections was performed (Williams, 1977; Weibel, 1979). For each time interval, 3–5 ultrathin sections taken from the 2 blocks of the pancreas of each mouse were placed on 400 mesh grids. The section which was the most technically adequate and most clearly stained was selected. Generally, the grid pattern defined 2–3 complete section windows, each of which was photographed at the centre to provide prints for measurements. Such systematic sampling (in which 2–5 cell profiles appear in each print) gives a very low standard error ($< 10\%$) for the measurements. At each time interval, 4–6 prints from each of the 5 mice in each treatment group, were analysed and the results pooled (i.e. for each time interval at least 24 prints/treatment group).

Volume fraction (Vv) was estimated by superimposing a single square lattice grid ($d = 1$ cm, i.e. 1 point/cm^2) over the micrograph (Williams, 1977; Hammel et al. 1987, 1989). The total number of points over each tissue compartment was counted (Pc_i, $i = 1,2,3 \ldots\ldots n$). Total cell (cell) and nucleus (nuc) profile areas were also estimated using point counting ($Pcell_i$ and $Pnuc_i$, respectively). Thus, the cytoplasmic (cyto) area, $Pcyto_i$, was calculated as the difference between these 2 measurements ($Pcyto_i = Pcell_i - Pnuc_i$). $Pcyto_i$

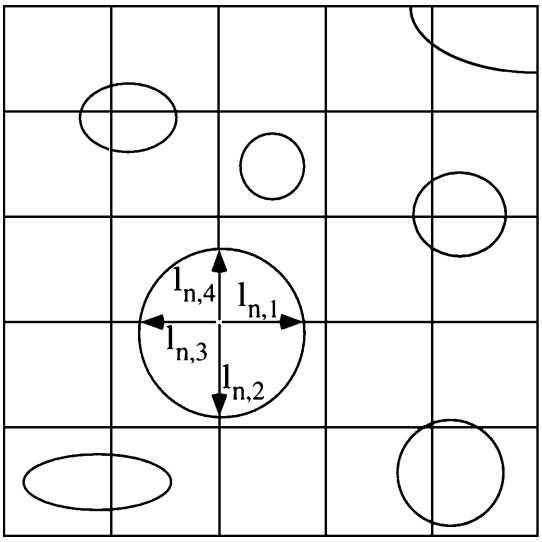

Fig. 1. Diagram to illustrate the determination of star volume showing the point-sampling of convex vesicles. A test system is overlaid on the micrograph. Organelle profiles are point-sampled. Wherever an intersection crosses a particle profile the 4 line intercepts (l_n) are measured, thus $v_* = (4\pi/3)(\overline{l_n^3})$.

was used as a reference and therefore $Vv = \Sigma Pc_i / \Sigma Pcyto_i$. Mitochondrion star volume (v_*) was estimated as explained in detail by Gundersen & Jensen (1985). Briefly, a single square lattice grid (d = 0.5 cm, i.e. 0.25 point/cm^2) was superimposed on the micrograph (Fig. 1). Wherever an intersection crossed the mitochondrion profile (Fig. 1) the 4 line intercepts (l_n) were measured, thus $v_* = (4\pi/3)(\overline{l_n^3})$. This methodology was used since we had to characterise a population of 3-dimensional components composed of multiple substructures and different volumes. By analysing the star volume of the structures (as revealed in transmission electron micrograph) using a volume-weighted method free from assumptions of structure, we were able to detect significant structural volume changes not visible to the eye. RER surface density (Sv) was calculated by counting the number of intersections (I_i) of the RER boundaries with the grid lines, thus, $Sv = \Sigma I_i / d\Sigma Pc_i$ (Williams, 1977). Data are presented as mean $\pm$S.D. between animals. Differences of total numbers between groups were judged by 2-tailed Student's *t* test and the Mann-Whitney U-test.

RESULTS

Ultrastructure of resting and pilocarpine-stimulated pancreatic acinar cells

The ultrastructure of normal and pilocarpine-treated mouse pancreatic acinar cells after 2 and 8 h following injection, is shown in Figure 2. The cellular granule content of pilocarpine-affected mice 2 h following activation is markedly diminished. The RER seems to undergo no major morphological change. Autophagosomal material of heterogeneous electron density is noticed in the degranulated cells (Fig. 2). The autophagic vacuoles contain recognisable cytoplasmic structures such as mitochondria and fragments of RER. The cell nucleus electron density of the 2 h groups seems to be less when compared with the 8 h cell nucleus. At 4 h following activation (Fig. 3) some mature granules are noticed near the acinar lumen. The mitochondrial profiles are longer and more electron dense when compared with the 2 and 8 h groups.

Nuclear changes following cell degranulation

The kinetics of nuclear volume changes following pilocarpine injection are summarised in Figure 4. Nuclear size gradually increases following activation approaching a maximal volume 2 h after degranulation. Segregation of the nucleus into 2 compartments, consisting of electron dense masses (heterochromatin and nucleolus-synthesis zone within the nucleus) and an electron transparent zone (euchromatin), reveals that the volume of the electron dense masses is constant throughout the whole 27 h of follow-up, whereas the electron transparent masses are the major contributor to nucleus volume changes. Before degranulation the volume is about 74 ± 6 μm^3 while at 2–4 h it is increased by about 70% (132 ± 9 μm^3 and 127 ± 9 μm^3 respectively, $P < 0.05$).

Two hours after pancreatic acinar cell degranulation an increased proportion of autophagosome is noted

Examination of the volume of autophagosomal structures in resting pancreatic acinar cells and in those studied after pilocarpine stimulation (Fig. 5) indicated that autophagosome content in resting (control) cells was significantly lower (9.1 ± 2.1 μm^3) than that observed in the 2 h group cells (77.4 ± 18.2 μm^3, $P < 0.001$ vs control value). This change in mean autophagosome volume after pilocarpine injection primarily reflected a greatly increased proportion of autophagic vacuole profiles containing recognisable cytoplasmic structures such as mitochondria, granule profiles and fragments of RER. The change in autophagosome volume in cells stimulated with pilocarpine, which persisted for a short time after stimulation, had resolved in cells examined 27 h after administration of the agent. Thus the mean volume for autophagosome observed 4–27 h after pilocarpine

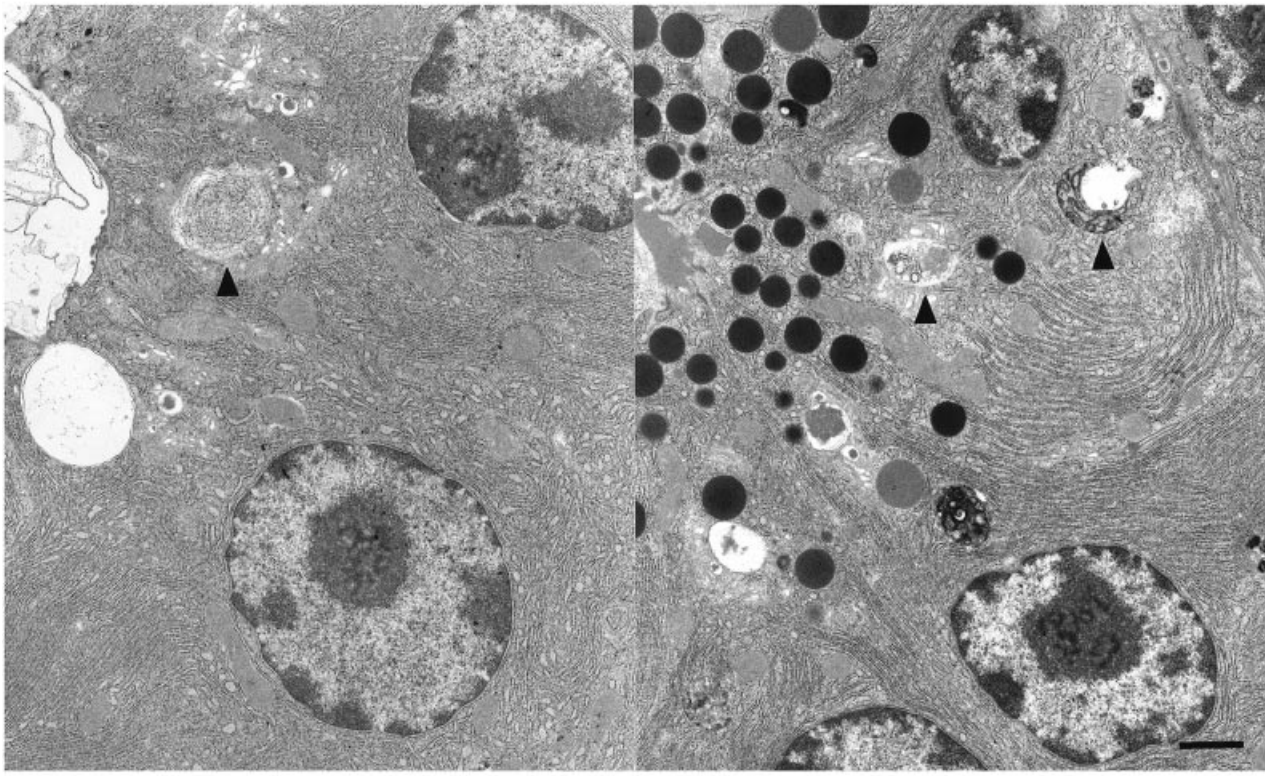

Fig. 2. Electron micrograph composite of pancreatic acinar cells following pilocarpine injection. Mitochondria are scattered within the cells. Two h after pilocarpine administration (left panel) the cell contains almost no electron dense granules. The RER is the most abundant compartment and autophagosomal activity is noted (arrowheads). At a later interval (8 h-right panel) the cell nucleus is smaller and seems to have more electron dense material. Numerous mature granules are observed and occupy a large fraction of the cytoplasm. Bar, 1 μm.

was almost constant and similar to the corresponding control value (8.3 ± 2.0 μm^3, 27 h; vs 0,4–17 h value).

RER structural changes

During the first few hours following activation, there was a significant decrease in gross RER volume reaching a diminution level (4 h after stimulation) of 54% as compared with the volume in control cells (before stimulation, 1830 ± 551 μm^3, at 4 h 849 ± 161 μm^3; $P < 0.01$) (Fig. 6). The change in RER content in cells stimulated with pilocarpine, which persisted for at least 17 h after stimulation, had almost resolved in cells examined 27 h after administration of the agent (reaching a value of 1552 ± 295 μm^3). Interestingly, following maximal autophagosomal activity, gross RER surface membrane content is reduced significantly by about 45% (Fig. 6, inset).

Changes in the size of mitochondria after pilocarpine injection

We then point-sampled the mitochondria profile observed at multiple intervals after pilocarpine injection and calculated the corresponding true volume-weighted mean volume. The results were expressed as the actual mean volumes of a mitochondrion as a function of time after pilocarpine injection (Fig. 7, lower panel). The results indicate that pilocarpine-induced secretion was followed, at 1–4 h, by a marked ($\times 3$) increase in the mean volume of the mitochondria in the cell cytoplasm (before degranulation 0.178 ± 0.028 while at 4 h peak value 0.535 ± 0.109 μm^3, $P < 0.001$). The mean volume of the mature granules (Lew et al. 1994) had detectably decreased 8–27 h after pilocarpine ($P < 0.05$ vs 17 h value) and exceeded the control value (by 50–100%), at 17 or 27 h after stimulation ($P < 0.05$ vs before cell activation-control and 1 h groups). These results are consistent with the findings expected if mitochondria change their shape and volume as a physiological reaction to intracellular levels of ATP or ions such as Na^+ or Ca^{2+}.

In addition we have also estimated the mitochondrial volume fraction. The results indicate that the mitochondria reach their maximal total gross volume content within the cell 8 h after cell activation (Fig. 7, upper panel). The graph appears to be bimodal. The first mode at 2 h (before cell activation

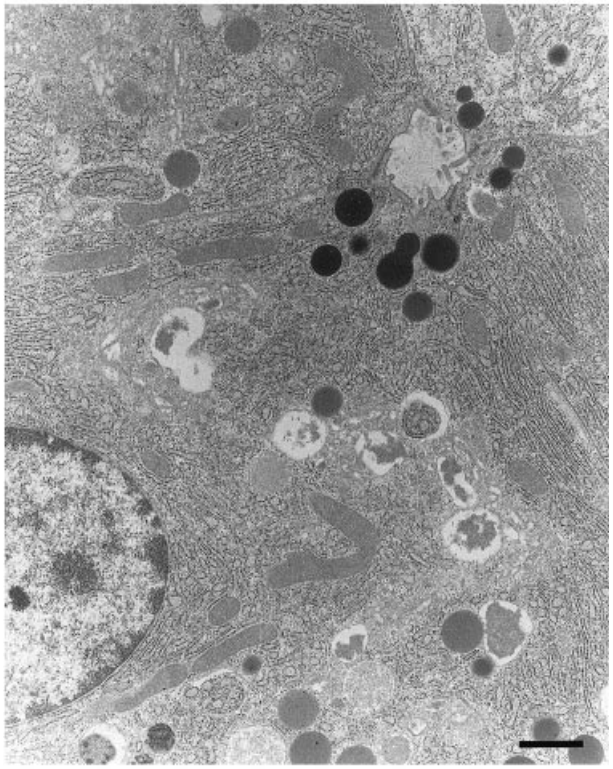

Fig. 3. Electron micrograph of pancreatic acinar cells 4 h following pilocarpine injection. Long mitochondria are scattered within the cells. The electron dense granules are small and few in number, 1 dumbbell-shaped granule is noted near the acinar lumen suggesting granule-granule fusion. Bar, 1 μm.

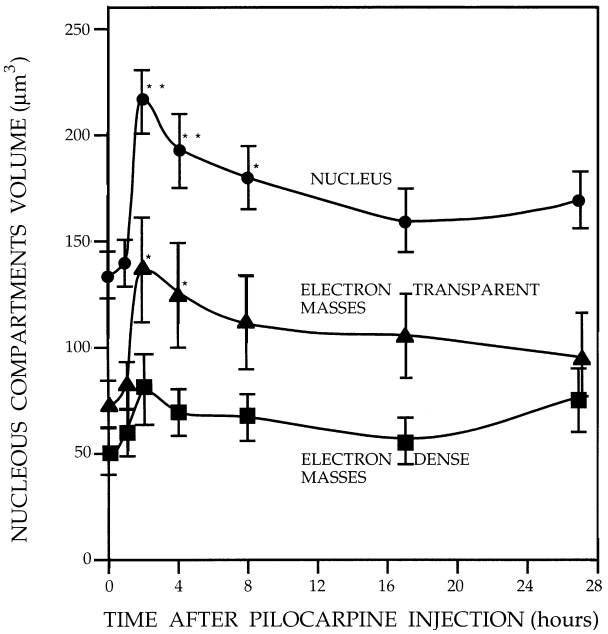

Fig. 4. Volume of nucleus of mouse pancreatic acinar cells in fasted mice before (0 h) or at various intervals after administration of pilocarpine. * or ** = $P < 0.05$ or 0.01 vs 0 h (baseline) value.

$Vv = 0.027 \pm 0.03\ \mu m^3/\mu m^3$, while at 2 h $Vv = 0.040 \pm 0.05\ \mu m^3/\mu m^3$; $P < 0.05$). At 4 h after cell activation the trough value of Vv is decreased to

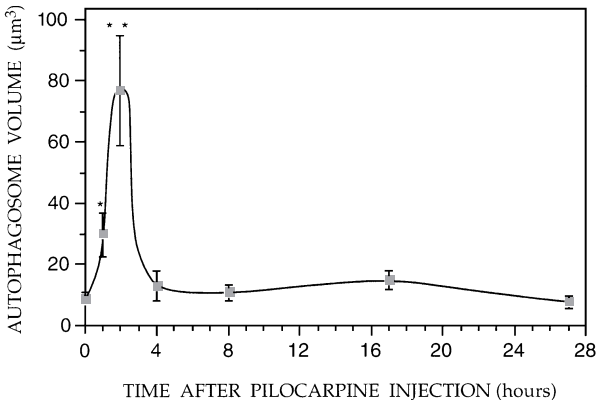

Fig. 5. Autophagosomal activity in mouse pancreatic acinar cells after administration of pilocarpine. * or ** = $P < 0.05$ or 0.01 vs 0 h (baseline, fasted mice before injection) value.

$0.034 \pm 0.04\ \mu m^3/\mu m^3$ and then increases at 8 h to a maximal Vv of $Vv = 0.057 \pm 0.06\ \mu m^3/\mu m^3$. At 17–27 h following degranulation the Vv (0.024–$0.026\ \mu m^3/\mu m^3$) is similar to the values before degranulation. If we assume that the mitochondrial star volume is similar to the number average value (usually it is about 10% higher) then we may calculate the ratio Vv/μm which is an estimate of the mitochondrial number density. Thus before degranulation and up to 8 h after, it is about 0.11–0.16 mitochondria/μm^3 while at 8 and 17–27 h it is decreased (0.90 and 0.68 mitochondria/μm^3 respectively).

DISCUSSION

The data presented in this communication describe a morphometric follow-up of size changes of some of the ultrastructural compartments within the acinar cells which are involved in secretory granule formation and secretion. In previous studies we have documented that following degranulation the mechanism of granule synthesis is activated to form granules of quantal size, the unit granule model. The unit granules fuse with other granules and thus result in granules which are multimers of the unit granule (Hammel et al. 1987, 1989). During the formation of unit granules, membrane is recycled. For secretory acinar cells we have estimated the membrane recycling to approximate to 95% (Lew et al. 1994). Thus, in addition to the central machinery involved in granule formation, we decided to investigate ultrastructural changes of other cellular compartments involved in granule formation. Previously we have demonstrated that pilocarpine induced a marked diminution in the Vv of MGs (92% less than control levels at 2 h after stimulation, returning to 128% of control levels by 17 h after stimulation) (Lew et al. 1994). In this study, we have used a morphometric approach to analyse an

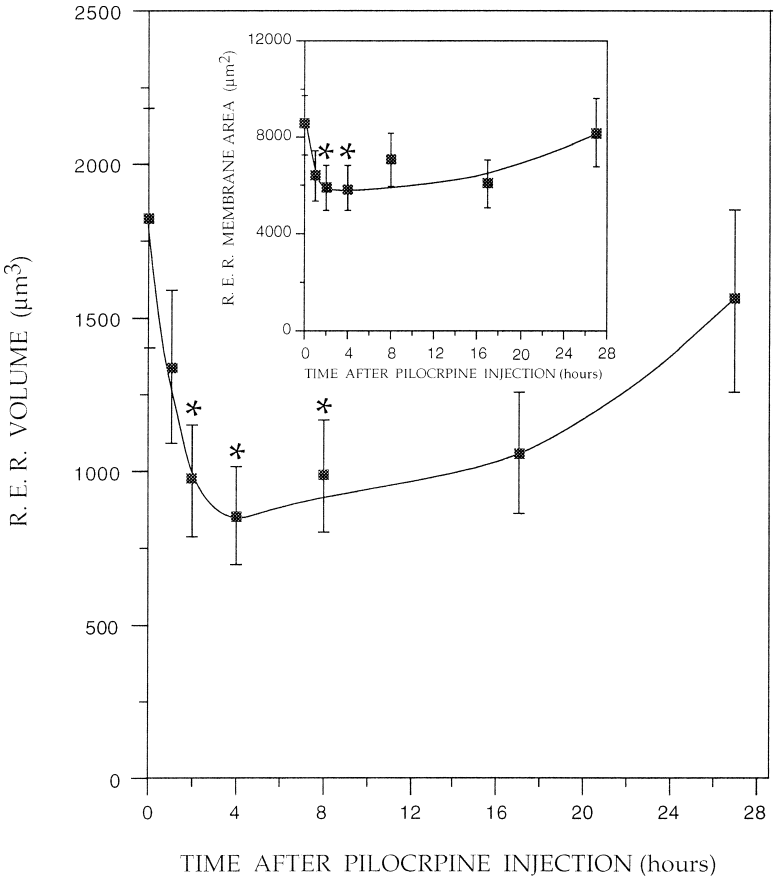

Fig. 6. Volume and surface area (inset) of RER of mouse pancreatic acinar cells in fasted mice before (0 h) or at various intervals after administration of pilocarpine. * or ** = $P < 0.05$ or 0.01 vs 0 h (baseline) value.

earlier step in the process of protein secretion. We selected a well-established model of cell secretion in vivo: pilocarpine-induced degranulation of pancreatic acinar cells (Covell, 1928; Nevalainen, 1970), and fixed pancreases for morphometric recognition before and at various intervals of up to 27 h after stimulation with pilocarpine. Our objectives were to characterise quantitatively pilocarpine-induced changes in important cellular compartments which are associated with the granule biogenesis, i.e. nucleus, RER, mitochondria and autophagosomes. Other compartments (e.g. Golgi complex, progranules, mature granules) have been examined in our previous studies (Weintraub et al. 1992; Lew et al. 1994).

It is believed that the granule membrane is almost entirely withdrawn into the cell by endocytosis (Kalina & Robinovitch, 1975; Farquhar & Palade, 1981; Oliver, 1982; Cope, 1983; Jena et al. 1994). Much interest has been shown in intracellular autophagy, the major pathway of lysosomal degradation of endogenous intracellular macromolecules and structures. By far the most studied version of the process is termed macroautophagy, in which large cytoplasmic contents are encircled by a membrane of special lysosomes (Oliver, 1982). The term autophagic vacuole is used as a common morphological term for autophagosomes when their enzyme content is uncertain in electron micrographs. Upon fusion, an autophagic vacuole arises within which the degradation is detectable both morphologically and biochemically. Autophagy is a 3-step process in which parts of the cytoplasm are segregated by membranes to form autophagosomes as the first step. These then gain acid hydrolases and are finally converted in this way into a final form of autophagic vacuoles in which lysosomal degradation takes place (also defined as an autophagolysosome). Williams & Cope (1981) suggested that the resultant degraded membranes form a membrane 'cryptic pool'. The actual size of the autophagic vacuole compartment is obviously dependent on the velocity of these main steps (Geuze & Kramer, 1974; Dunn, 1990). Our morphometric results indicate that on termination of degranulation (1 h after degranulation; Lew et al. 1994) initial significant structures characteristic of macroautophagy appear, demonstrating highest peak activity 1 h later (current work). If autophagosomal activity is a marker of membrane withdrawal, then the peak

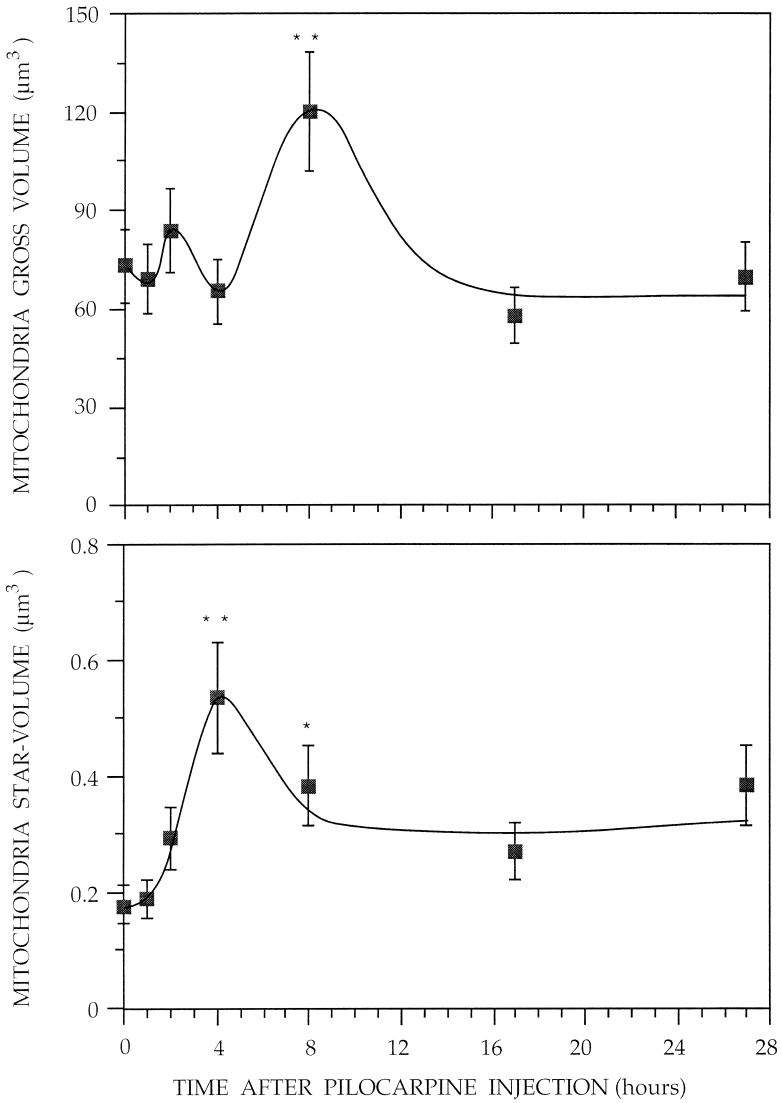

Fig. 7. Morphometric characteristics of pancreatic mitochondria. The upper panel indicates the volume fraction data and the lower panel the mean star volume of a single mitochondrion. * or ** = $P < 0.05$ or 0.01 vs 0 h (baseline) value.

period of maximal autophagocytosis activity is 2 h following cell activation. It is probably terminated less than 4 h later in our system (current work). In a similar rat system, Nevalainen (1970) demonstrated that the peak activity of the numerical density of vesicles appeared to correspond to the time that cytoplasmic volume is at its lowest level, similar to our current data. In a different system, also using a morphometric approach, Rez et al. (1996) have demonstrated that pancreatic acinar cells react to vinblastine biphasically, i.e. 2 expansion phases of the autophagic vacuole compartment, the first in the 0–90 min and the second in the 2–8 h postinjectional period. This biphasic observation confirms previous results found by Oliver (1982) which suggest that 2 separate and distinct endocytic pathways exist in exocrine acinar cells: one involves membrane retrieval from the apical cell surface and the other is a stimulation-dependent process at the lateral and basal cell surfaces. We have observed that minimal gross RER volume is achieved at 4 h following injection. Since RER volume is important for secretory protein synthesis and processing, low RER volume at that time-point indicates that changes in ionic activity and protein content may probably contribute to the RER size changes.

The variations in mitochondrial gross volume and size analysed during the 27 h span seem to be different when compared with the other variables studied. The gross mitochondrial volume was bimodal. The first nonsignificant peak correlates with maximal autophagosomal activity (2 h) and the second ($P < 0.01$) at 8 h following activation. However, the change in the volume of a single mitochondrion (estimated as star volume) was unimodal with a peak value at 4 h ($P < 0.01$). Star volume is a volume-weighted mean

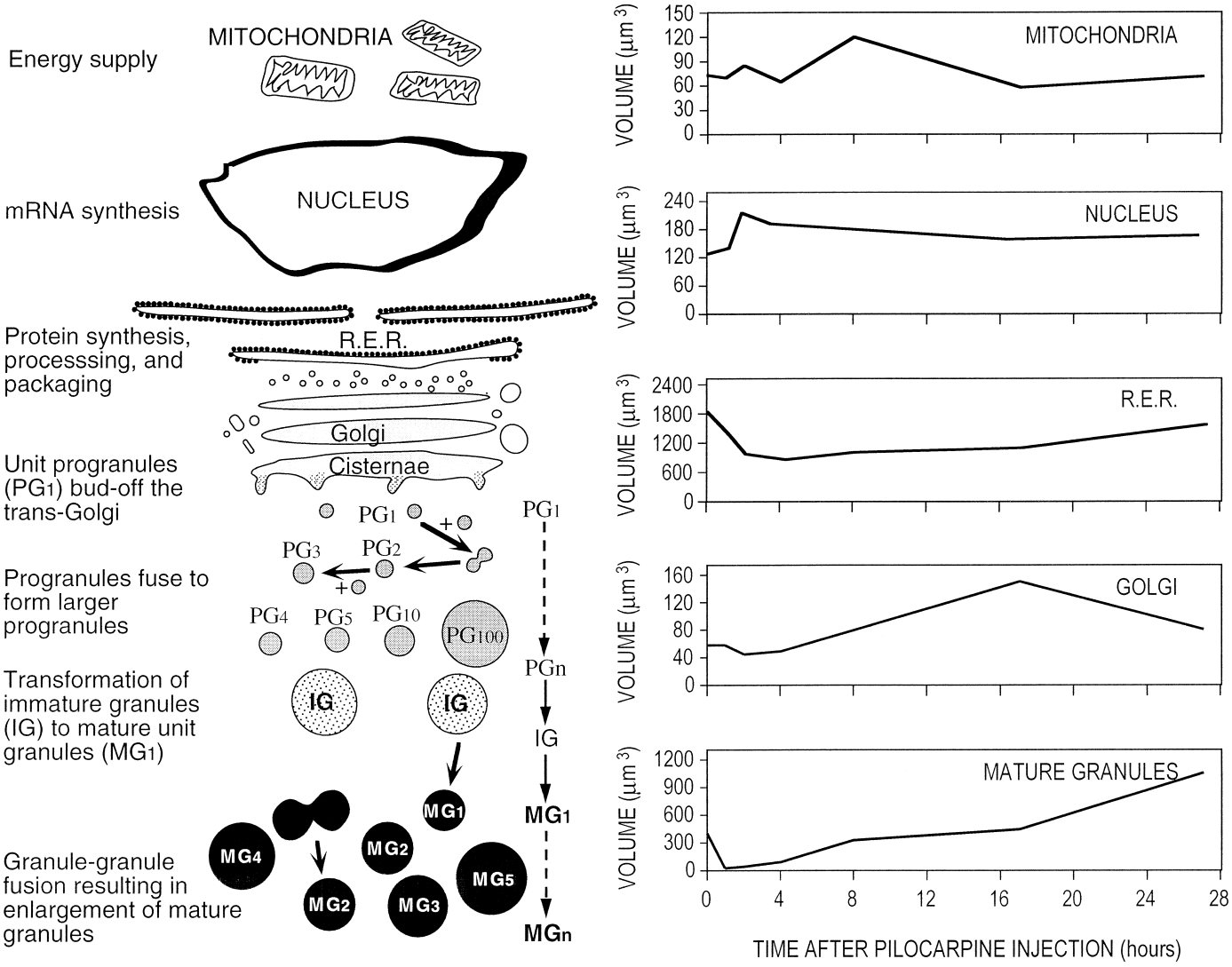

Fig. 8. Diagram illustrating the major kinetic steps in cellular events during the regranulation process in pancreatic acinar cell.

average and therefore highly sensitive to mitochondrial size distribution. However, gross volume is a result of parameters which are independent of mitochondrial size distribution. Thus we may suggest only that the gross volume summarises the data on total mitochondrial volume within a single cell, while the star volume indicates only that 4 h following injection there are some significant large mitochondria. Thus, the size increase and mitochondrial accumulation suggest that the long mitochondria (Fig. 3) represent mitochondrial growth and multiplication. In addition, it is well accepted that mitochondrial size reflects activity state. The data indicate that mitochondria tended to become large during the increase in protein transport from the RER to the Golgi apparatus and when recovery of RER volume occurred. If mitochondrial volume indicates the state of energy production, this energy supply may be necessary for the increase in the amount of RER necessary for regranulation to occur. Previously we have documented that significant granule synthesis starts at 4 h with a constant rate of about 4–6 unit-granule. min^{-1} $cell^{-1}$. The Golgi compartment volume was maximal at 17 h following degranulation (Lew et al. 1994). Thus, the energy requirements are mainly for protein synthesis, processing and packaging.

In a morphometric study of 24 h variations in subcellular structures of the rat pancreatic acinar cell, Uchyama & Saito (1982) found that mitochondrial area profiles vary with the time of day. The change in mitochondrial profiles seemed to coincide with that of the activity of protein transport from the RER to the Golgi apparatus. That is at 04.00 h, when the cells are postulated to be inactive in protein transport, mitochondria often exhibited a slender, elongated form. Moreover, mitochondria tended to become voluminous during the increase in protein transport from the RER to the Golgi apparatus. On the other hand, at midnight, when rapid recovery of RER area occurred, mitochondrial area exhibited a maximal value. Thus it was concluded that if the mitochondrial profiles and area indicate the state of energy production, this energy supply may be necessary for the increase in the amount of RER.

From these variations in the subcellular structures, it is possible to divide the regranulation span into 3 stages (Fig. 8). (1) Membrane remodelling stage (0–2 h): during this period the volume of the RER and secretory granules is greatly decreased. (2) Intermediate stage (2–4 h): during this stage, as a result of the rapid release of zymogen granules from the acinar cells, the nucleus exhibits a significant volume increase of the synthesis zone. The amount of RER is markedly decreased. Mitochondria start to change in volume. (3) Restitution: granule synthesis and accumulation stage (after 4 h, this event proceeds evenly over the next 12 h period). From the morphological point of view almost no autophagosomal activity is observed. The Golgi complex increases in size to its initial volume (it may imply the active state of secretory protein synthesis). There is probably a demand for energy as demonstrated by the mitochondrial size changes.

ACKNOWLEDGEMENTS

The authors wish to thank Dr T. Weinstein and Professor E. Skutelsky for critical reading of the manuscript and valuable advice and discussion. In addition we wish to thank Edna Zolin for her kind help in the preparation of the manuscript. Financial support for this work was received by the Tel Aviv University Basic Research Foundation and by a grant from the Chief Scientist, Ministry of Health, Israel

REFERENCES

AUGHTEEN AA, COPE GH (1987) Changes in the size and number of secretion granules in the rat exocrine pancreas induced by feeding or stimulation in vitro. A morphometric study. *Cell and Tissue Research* **249**, 427–436.

CASTLE JD, CAMERON RS, ARVAN P,VON ZASTROW M, RUDNICK G (1987) Similarities and differences among neuroendocrine, exocrine and endocytic vesicles. *Annals of New York Academy of Sciences* **493**, 448–460.

COPE GH (1983) Exocrine glands and protein secretion: a stereological viewpoint. *Journal of Microscopy* **131**, 187–202.

COVELL WP (1928) A microscopic study of pancreatic secretion in the living animal. *Anatomical Record* **40**, 213–224.

DARNELL J, LODISH H, BALTIMORE D (1990) Plasma–membrane, secretory and lysosome proteins: biosynthesis and sorting. In *Molecular Cell Biology*, 2nd edn, pp. 639–680. New York: Scientific American Books.

DUNN Jr WA (1990) Studies on the mechanism of autophagy: formation of the autophagic vacuole. *Journal of Cell Biology* **110**, 1923–1933.

FARQUHAR MG (1985) Progress in unraveling pathways of Golgi traffic. *Annual Review of Cell Biology* **1**, 447–488.

FARQUHAR MG, PALADE GE (1981). The Golgi apparatus (complex) (1954–1981)—from artifact to center stage. *Journal of Cell Biology* **91**, 77s–103s.

GEUZE JJ, KRAMER MF (1974). Function of coated membranes and multivesicular bodies during membrane regulation in stimulated exocrine pancreas cells. *Cell and Tissue Research* **156**, 1–20.

GUNDERSEN HJG, JENSEN EB (1985) Stereological estimation of the volume-weighted mean volume of arbitary particles observed on random sections. *Journal of Microscopy* **138**, 127–142.

HAMMEL I, DVORAK AM, PETERS SP, SCHULMAN ES, DVORAK HF, LICHTENSTEIN LM et al. (1985) Differences in the volume distributions of human lung mast cell granules and lipid bodies: evidence that the size of these organelles is regulated by distinct mechanisms. *Journal of Cell Biology* **100**, 1488–1492.

HAMMEL I, DVORAK AM, FOX P, SHIMONI E, GALLI SJ (1998) Defective cytoplasmic granule formation. II. Differences in patterns of radiolabeling of secretory granules in beige versus

normal mouse pancreatic acinar cells after [^{3}H]-glycine administration *in vivo*. *Cell and Tissue Research* **293**, 445–452.

HAMMEL I, DVORAK AM, GALLI SJ (1987). Defective cytoplasmic granule formation. I. Abnormalities affecting tissue mast cells and pancreatic acinar cells of beige mice. *Laboratory Investigation* **56**, 321–328.

HAMMEL I, LAGUNOFF D, KRÜGER P-G (1989). Recovery of rat mast cells after secretion: a morphometric study. *Experimental Cell Research* **184**, 518–523.

JENA BP, GUMKOWSKI FD, KONIECZKO EM, VON MOLLARD GF, JAHN R, JAMIESON JD (1994) Redistribution of a rab3-like GTP-binding protein from secretory granules to the Golgi complex in pancreatic acinar cells during regulated exocytosis. *Journal of Cell Biology* **124**, 43–53.

JENSEN EB, GUNDERSEN HJG (1985) The stereological estimation of moments of particle volume. *Journal of Applied Probability* **22**, 82–98.

JAMIESON JD, PALADE GE (1967) Intracellular transport of secretory proteins in the pancreatic exocrine cell. II. Transport to condensing vacuoles and zymogen granules. *Journal of Cell Biology* **34**, 597–615.

JAMIESON JD, PALADE GE (1971) Condensing vacuole conversion and zymogen granule discharge in pancreatic exocrine cells : metabolic studies. *Journal of Cell Biology* **48**, 503–522.

KALINA M, ROBINOVITCH R (1975) Exocytosis couples to endocytosis of ferritin in parotid acinar cells from isoprenalin stimulated rats. *Cell and Tissue Research* **163**, 373–382.

LEBLOND CP (1981) The life history of cells in renewing systems. *American Journal of Anatomy* **160**, 114–158.

LEW S, HAMMEL I, GALLI SJ (1994) Cytoplasmic granule formation in mouse pancreatic acinar cells. I. Quantitative recognisis of changes in the size distribution of progranules and mature granules after pilocarpine-induced secretion. *Cell and Tissue Research* **278**, 327–336.

NEVALAINEN TJ (1970) Effects of pilocarpine stimulation on rat pancreatic acinar cells. *Acta Pathologica et Microbiologica Immunologica Scandinavica* (*Supplementum*) **210**, 1–70.

OKANO Y, NAKAMURA T (1965) Electron microscopic observations on exocrine pancreas cells in mice following the injection of pilocarpine. *Journal of Electron Microscopy* (*Tokyo*) **14**, 242–243.

OLIVER C (1982) Endocytic pathways at the lateral and basal cell surfaces of exocrine acinar cells. *Journal of Cell Biology* **95**, 154–161.

PFEFFER SR, ROTHMAN JE (1987) Biosynthetic protein transport and sorting by the endoplasmic reticulum and Golgi. *Annual Review of Biochemistry* **56**, 829–859.

REZ G, CSAK J, FELLINGER E, LASZLO L, KOVACS AL, OLIVA O et al. (1996) Time course of vinblastine-induced autophagocytosis and changes in the endoplasmic reticulum in murine pancreatic acinar cells: a morphometric and biochemical study. *European Journal of Cell Biology* **71**, 341–350.

SCHROEDER F, JEFFERSON JR, KIER AB, KNITTEL J, SCALLEN TJ, WOOD WG et al. (1991) Membrane cholesterol dynamics: cholesterol domains and kinetic pools. *Proceeding of the Society of Experimental Biology and Medicine* **196**, 235–252.

SEVERS NJ, ROBENEK H (1983) Detection of microdomains in biomembranes. An appraisal of recent developments in freeze-fracture cytochemistry. *Biochimica et Biophysica Acta* **737**, 373–408.

UCHIYAMA Y, SAITO K (1982). A morphometric study of 24-hour variations in subcellular structures of the rat pancreatic acinar cell. *Cell and Tissue Research* **226**, 609–620.

UNDERWOOD EE (1970) *Quantitative Stereology*. Reading, MA: Addison-Wesley.

WATARI N, BABA N (1968). Several findings on the fine structural alterations of the exocrine pancreas after the administration of some chemicals. *Journal of Electron Microscopy* (*Tokyo*) **17**, 327–341.

WEIBEL ER (1979) *Stereological Methods*, *vol 1. Practical Methods for Biological Morphometry*, and vol 2. *Theoretical Foundations*. London: Academic Press.

WEINTRAUB H, ABRAMOVICI A, AMICHAI D, ELDAR T, BEN-DOR L, PENTCHEV PG et al. (1992) Morphometric studies of pancreatic acinar granule formation in NCTR-Balb/c mice. *Journal of Cell Science* **102**, 141–147.

WILLIAMS MA (1977) Stereological techniques. In *Quantitative Methods in Biology*, pp. 5–84. New York: North-Holland.

WILLIAMS MA, Cope GH (1981) Membrane dynamics in the parotid acinar cell during regranulation: a stereological study following isoprenaline-induced secretion. *Anatomical Record* **199**, 389–401.